

Lepton flavor violating decays of vector mesons in the MRSSM*

Ke-Sheng Sun (孙科盛)^{1†} Wen-Hui Zhang (张文慧)^{2,3,4‡} Jian-Bin Chen (陈建宾)^{5§}

Hai-Bin Zhang (张海斌)^{2,3,4¶} Qi-geng Yan (闫其庚)^{1‡}

¹Department of Physics, Baoding University, Baoding 071000, China

²Department of Physics, Hebei University, Baoding 071002, China

³Key Laboratory of High-Precision Computation and Application of Quantum Field Theory of Hebei Province, Baoding 071002, China

⁴Research Center for Computational Physics of Hebei Province, Baoding 071002, China

⁵College of Physics and Optoelectronic Engineering, Taiyuan University of Technology, Taiyuan 030024, China

Abstract: In this study, we analyze the rare decays of the neutral vector mesons J/ψ and $\Upsilon(nS)$ in the scenario of the minimal R-symmetric supersymmetric standard model using the effective Lagrangian method. The predicted branching ratios are dominated by the mass insertion parameters δ^{ij} , *i.e.*, the off-diagonal inputs, and the contributions of different parts are comparable. Taking into account the experimental constraints on the mass insertion parameters, the predicted branching ratios for the most promising processes $\Upsilon(nS) \rightarrow l\tau$ are ten orders of magnitude smaller than the present experimental bounds.

Keywords: MRSSM, lepton flavor violating

DOI: 10.1088/1674-1137/acd3da

I. INTRODUCTION

It is well known that lepton flavor violating (LFV) decays, such as $l_1 \rightarrow l_2\gamma$, $l_1 \rightarrow 3l_2$, $\mu - e$ conversion, $h \rightarrow l_1l_2$, and $\tau \rightarrow Pl_1$, are strongly suppressed by small masses of neutrinos in the standard model (SM), in which the neutrino oscillations (the masses and the mixing) are accommodated. In the SM with three massive neutrinos, the predicted branching ratios (BRs) of the LFV decays of the vector meson V are under 10^{-50} [1], and this is far below the current experimental sensitivity. Nevertheless, in many new physics scenarios beyond the SM, the branching ratios of the LFV decays can be adjusted to be within the current experimental range; this is the case for the grand unified models [2–4], the two Higgs doublet models [5], the supersymmetric models [6], and the left-right symmetry models [7–9]. The results show that, in various SM extensions, the predicted $\text{BR}(V \rightarrow l_1l_2)$ can be within the range of the current or future experiments [1, 10–15]. The LFV decays of neutral vector mesons can also be studied in a model-independent manner [16–22],

which can be used to obtain the constraints on the Wilson coefficients.

Using a sample of about 10 billion J/ψ events collected by the BESIII detector [23, 24], the BESIII collaboration reported their results for the LFV decays of J/ψ . The upper limits on $\text{BR}(J/\psi \rightarrow e\mu)$ and $\text{BR}(J/\psi \rightarrow e\tau)$ were 4.5×10^{-9} and 7.5×10^{-8} at the 90% confidence level (CL), improving over the previous limits by one and two orders of magnitude [25, 26], respectively. Using the collected 158 million $\Upsilon(2S)$ events, the LFV decays of the neutral vector meson $\Upsilon(1S)$ have been detected at the Belle detector at the KEKB e^+e^- collider [27]. The estimated upper limit on the BR of $\Upsilon(1S) \rightarrow \mu\tau$ was 2.7×10^{-6} , which is 2.3 times more stringent than the previous result [28]. The Belle collaboration also performed the first search for $\Upsilon(1S) \rightarrow e\mu$ and $\Upsilon(1S) \rightarrow e\tau$ and the estimated upper limits were 3.9×10^{-7} and 2.7×10^{-6} , respectively. Using 118 million $\Upsilon(3S)$ samples collected by the BABAR detector at the PEP-II collider at SLAC, the BABAR collaboration set the upper limit on the LFV decay $\text{BR}(\Upsilon(3S) \rightarrow e\mu)$ at 3.6×10^{-7} , at the 90% CL [29]. In

Received 3 February 2023; Accepted 10 May 2023; Published online 11 May 2023

* Supported by the Natural Science Foundation of Hebei Province (A2022104001, A2022201017), the Shanxi Scholarship Council of China (2021-31), the youth top-notch talent support program of the Hebei Province, and the Foundation of Baoding University (2018Z01)

[†] E-mail: sunkesheng@bdu.edu.cn

[‡] E-mail: 1564070519@qq.com

[§] E-mail: chenjianbin@tyut.edu.cn

[¶] E-mail: hbzhang@hbu.edu.cn

[‡] E-mail: yanqigeng@bdu.edu.cn



Content from this work may be used under the terms of the Creative Commons Attribution 3.0 licence. Any further distribution of this work must maintain attribution to the author(s) and the title of the work, journal citation and DOI. Article funded by SCOAP³ and published under licence by Chinese Physical Society and the Institute of High Energy Physics of the Chinese Academy of Sciences and the Institute of Modern Physics of the Chinese Academy of Sciences and IOP Publishing Ltd

Table 1, we provide a summary of the current limits on the LFV decays of the neutral vector meson V ($V = J/\psi$, $\Upsilon(nS)$, ϕ).

In the present work, we analyze the LFV decays $V \rightarrow l_1 l_2$ in a model that contains the continuous R-symmetry [32, 33] and is called the minimal R-symmetric supersymmetric standard model (MRSSM) [34]. The gauge symmetry of the MRSSM is the same as those of the SM and MSSM. R-symmetry forbids Majorana gaugino masses, and the MRSSM contains Dirac gauginos and the gauge/gaugino sector is an $N = 2$ supersymmetric theory. In the MRSSM, the μ term, A terms and the left-right mixings in the squark and slepton mass matrices, which usually exist in the MSSM, are also absent. In the MSSM there is a $\tan\beta$ -enhancement for the muon anomalous magnetic dipole moment a_μ [35, 36] and a similar enhancement for the predictions of $\text{BR}(\mu \rightarrow e\gamma)$ and $\text{CR}(\mu - e, \text{nucleus})$ [37]. However, the $\tan\beta$ -enhancement for these observables does not exist in the MRSSM since there are no Majorana gaugino masses and no μ term [38]. The branching ratios of the LFV processes are affected by the off-diagonal inputs of the matrices m_l^2 and m_τ^2 . Several references to the phenomenology of the MRSSM are provided [38–56].

A brief introduction to the MRSSM is provided in Sec. II, and the notation for the operators and their corresponding Wilson coefficients are also given in that section. The numerical comparison of the different models is described in Sec. III. Section IV lists our conclusions.

II. THE MODEL

In this section, we firstly provide a simple introduction to the MRSSM. Similar to the SM and MSSM, the gauge symmetry of the MRSSM is $SU(3)_C \times SU(2)_L \times U(1)_Y$. The spectrum of fields in the MRSSM contains the standard MSSM matter, the Higgs and gauge superfields augmented by chiral adjoints \hat{S} , \hat{T} , \hat{O} and two R -Higgs iso-doublets. The R -charges of the superfields and the corresponding bosonic and fermionic components in the MRSSM are given in Table 2. The most general form of the superpotential in the MRSSM takes the form of Ref. [39]

$$\begin{aligned} \mathcal{W}_{\text{MRSSM}} = & \Lambda_d \hat{R}_d \cdot \hat{T} \hat{H}_d + \Lambda_u \hat{R}_u \cdot \hat{T} \hat{H}_u \\ & + \lambda_d \hat{S} \hat{R}_d \cdot \hat{H}_d + \lambda_u \hat{S} \hat{R}_u \cdot \hat{H}_u \\ & - Y_d \hat{d} \hat{q} \cdot \hat{H}_d - Y_e \hat{e} \hat{l} \cdot \hat{H}_d \\ & + Y_u \hat{u} \hat{q} \cdot \hat{H}_u + \mu_d \hat{R}_d \cdot \hat{H}_d + \mu_u \hat{R}_u \cdot \hat{H}_u, \end{aligned} \quad (1)$$

where the dot ' \cdot ' refers to an $SU(2)$ contraction with the Levi-Civita tensor, the MSSM-like Higgs weak iso-doublets are \hat{H}_u and \hat{H}_d , the R -charged Higgs $SU(2)_L$ doublets are \hat{R}_u and \hat{R}_d , and μ_u and μ_d stand for the Dirac higgsino mass parameters. Y_e , Y_u and Y_d stand for the Yukawa couplings of a charged lepton, up quarks and down quarks, respectively. $\lambda_{u,d}$ and $\Lambda_{u,d}$ stand for the Yukawa-like trilinear terms that involve the singlet \hat{S} and triplet \hat{T} , and the triplet \hat{T} takes the form of

Table 1. Current experimental limits on the LFV decays of neutral vector mesons.

Decay	Limit	Experiment	Decay	Limit	Experiment
$J/\psi \rightarrow e\mu$	4.5×10^{-9}	BESIII (2022)[23]	$J/\psi \rightarrow e\tau$	7.5×10^{-8}	BESIII (2021)[24]
$J/\psi \rightarrow \mu\tau$	2.0×10^{-6}	BES (2004)[26]	$\Upsilon(1S) \rightarrow e\mu$	3.9×10^{-7}	BELLE (2022)[27]
$\Upsilon(1S) \rightarrow e\tau$	2.7×10^{-6}	BELLE (2022)[27]	$\Upsilon(1S) \rightarrow \mu\tau$	2.7×10^{-6}	BELLE (2022)[27]
$\Upsilon(2S) \rightarrow e\tau$	3.2×10^{-6}	BABAR (2010)[30]	$\Upsilon(2S) \rightarrow \mu\tau$	3.3×10^{-6}	BABAR (2010)[30]
$\Upsilon(3S) \rightarrow e\mu$	3.6×10^{-7}	BABAR (2022)[29]	$\Upsilon(3S) \rightarrow \mu\tau$	3.1×10^{-6}	BABAR (2010)[30]
$\Upsilon(3S) \rightarrow e\tau$	4.2×10^{-6}	BABAR (2010)[30]	$\phi \rightarrow e\mu$	2×10^{-6}	SND (2010)[31]

Table 2. The field content of the MRSSM.

Field	Superfield	R -charge	Boson	R -charge	Fermion	R -charge
Gauge vector	$\hat{g}, \hat{W}, \hat{B}$	0	g, W, B	0	$\tilde{g}, \tilde{W}, \tilde{B}$	+1
	\hat{l}, \hat{e}	+1	\tilde{l}, \tilde{e}_R^*	+1	l, e_R^*	0
Matter	$\hat{q}, \hat{d}, \hat{u}$	+1	$\tilde{q}, \tilde{d}_R^*, \tilde{u}_R^*$	+1	q, d_R^*, u_R^*	0
H -Higgs	$\hat{H}_{d,u}$	0	$H_{d,u}$	0	$\tilde{H}_{d,u}$	-1
R -Higgs	$\hat{R}_{d,u}$	+2	$R_{d,u}$	+2	$\tilde{R}_{d,u}$	+1
Adjoint chiral	$\hat{S}, \hat{T}, \hat{O}$	0	S, T, O	0	$\tilde{S}, \tilde{T}, \tilde{O}$	-1

$$\hat{T} = \begin{pmatrix} \frac{\hat{T}^0}{\sqrt{2}} & \hat{T}^+ \\ \hat{T}^- & -\frac{\hat{T}^0}{\sqrt{2}} \end{pmatrix}.$$

For the phenomenological studies, we take the soft breaking scalar mass terms [39]

$$\begin{aligned} V_{S,B,S} = & (B_\mu(H_d^- H_u^+ - H_d^0 H_u^0) + h.c.) \\ & + m_{H_u}^2 (|H_u^0|^2 + |H_u^+|^2) + m_{H_d}^2 (|H_d^0|^2 + |H_d^-|^2) \\ & + m_T^2 (|T^0|^2 + |T^-|^2 + |T^+|^2) \\ & + m_{R_u}^2 (|R_u^0|^2 + |R_u^-|^2) + m_{R_d}^2 (|R_d^0|^2 + |R_d^+|^2) \\ & + \tilde{u}_{L,i}^* m_{q,i,j}^2 \tilde{u}_{L,j} + \tilde{u}_{R,i}^* m_{u,i,j}^2 \tilde{u}_{R,j} + \tilde{d}_{L,i}^* m_{q,i,j}^2 \tilde{d}_{L,j} \\ & + \tilde{d}_{R,i}^* m_{d,i,j}^2 \tilde{d}_{R,j} + \tilde{\nu}_{L,i}^* m_{l,i,j}^2 \tilde{\nu}_{L,j} \\ & + \tilde{e}_{L,i}^* m_{l,i,j}^2 \tilde{e}_{L,j} + \tilde{e}_{R,i}^* m_{r,i,j}^2 \tilde{e}_{R,j} + m_S^2 |S|^2 + m_O^2 |O|^2. \end{aligned} \quad (2)$$

Due to the R -symmetry, the trilinear terms that contain the interaction between the slepton/squark and the Higgs boson are absent. The couplings involving the auxiliary D -fields to the adjoint scalars and the Dirac gaugino mass terms are included in the soft break terms, given by

$$\begin{aligned} V_{S,B,DG} = & M_D^W (\tilde{W}^a \tilde{T}^a - \sqrt{2} \mathcal{D}_W^a T^a) + M_D^g (\tilde{g} \tilde{O} - \sqrt{2} \mathcal{D}_g^a O^a) \\ & + M_D^B (\tilde{B} \tilde{S} - \sqrt{2} \mathcal{D}_B S) + h.c., \end{aligned} \quad (3)$$

where \tilde{W} , \tilde{g} , and \tilde{B} are the Weyl fermions, and M_D^W, M_D^g , and M_D^B stand for the masses of wino, gluino, and bino, respectively [39].

Because neutralinos are Dirac-type, the number of neutralinos in the MRSSM is two times higher than that in the MSSM. The neutralino mass matrix can be diagonalized by the two unitary matrices N^1 and N^2 , which are given by [39]

$$\begin{aligned} m_{\chi^0} = & \begin{pmatrix} M_D^B & 0 & -\frac{1}{2} g_1 v_d & \frac{1}{2} g_1 v_u \\ 0 & M_D^W & \frac{1}{2} g_2 v_d & -\frac{1}{2} g_2 v_u \\ -\frac{1}{\sqrt{2}} \lambda_d v_d & -\frac{1}{2} \Lambda_d v_d & -\mu_d^{\text{eff},+} & 0 \\ \frac{1}{\sqrt{2}} \lambda_u v_u & -\frac{1}{2} \Lambda_u v_u & 0 & \mu_u^{\text{eff},-} \end{pmatrix}, \\ \mu_{\{u,d\}}^{\text{eff},\pm} = & \pm \frac{1}{2} \Lambda_{\{u,d\}} v_T + \frac{1}{\sqrt{2}} \lambda_{\{u,d\}} v_S + \mu_{\{u,d\}}, \\ m_{\chi^0}^{\text{diag}} = & (N^1)^* m_{\chi^0} (N^2)^\dagger, \end{aligned} \quad (4)$$

where g_1 stands for the coupling constant for the $U(1)_Y$ sector, g_2 stands for the coupling constant for the $SU(2)_L$ sector, v_u stands for the nonzero vacuum expectation

value (vev) of the up-type Higgs doublet, v_d stands for the vev of the down-type Higgs doublet, and the ratio $\tan\beta = \frac{v_u}{v_d}$.

In light of the R -charge, each chargino can be separated into two parts: the χ -chargino (R -charge 1) and the ρ -chargino (R -charge -1). Thus, the number of charginos in the MRSSM is two times higher than that in the MSSM. It is noted that the ρ -chargino part has no effect on the LFV decays and we do not refer to this part in this paper. The χ -chargino mass matrix can be diagonalized by the two unitary matrices U^1 and V^1 , which are given by [39]

$$\begin{aligned} m_{\chi^\pm} = & \begin{pmatrix} M_D^W + g_2 v_T & \frac{1}{\sqrt{2}} \Lambda_d v_d \\ \frac{1}{\sqrt{2}} g_2 v_d & \mu_d^{\text{eff},-} \end{pmatrix}, \\ m_{\chi^\pm}^{\text{diag}} = & (U^1)^* m_{\chi^\pm} (V^1)^\dagger. \end{aligned} \quad (5)$$

As mentioned above, the off-diagonal terms of the slepton mass matrix are zero where the μ and A terms exist in the MSSM. The slepton/sneutrino mass matrix can be diagonalized by the unitary matrices Z^E and Z^V , respectively, which are given by [38]

$$\begin{aligned} m_{\tilde{e}}^2 = & \begin{pmatrix} (m_{\tilde{e}}^2)_{LL} & 0 \\ 0 & (m_{\tilde{e}}^2)_{RR} \end{pmatrix}, \\ m_{\tilde{\nu}}^2 = & \frac{1}{8} (g_1^2 + g_2^2) (v_d^2 - v_u^2) + g_2 v_T M_D^W - g_1 v_S M_D^B + m_l^2, \\ m_{\tilde{e}}^{2,\text{diag}} = & Z^E m_{\tilde{e}}^2 (Z^E)^\dagger, \\ m_{\tilde{\nu}}^{2,\text{diag}} = & Z^V m_{\tilde{\nu}}^2 (Z^V)^\dagger, \end{aligned} \quad (6)$$

where

$$\begin{aligned} (m_{\tilde{e}}^2)_{LL} = & \frac{1}{8} (g_1^2 - g_2^2) (v_d^2 - v_u^2) - g_1 v_S M_D^B \\ & - g_2 v_T M_D^W + \frac{1}{2} v_d^2 |Y_e|^2 + m_l^2 \\ (m_{\tilde{e}}^2)_{RR} = & \frac{1}{4} g_1^2 (v_u^2 - v_d^2) + 2 g_1 v_S M_D^B + \frac{v_d^2}{2} |Y_e|^2 + m_r^2. \end{aligned}$$

Compared with the MSSM, the last two terms in the sneutrino mass matrix are added in the MRSSM.

The off-diagonal terms of the up/down squark mass matrix are zero. The mass matrix for up/down squarks can be diagonalized by the unitary matrices Z^U and Z^D , respectively, which are given by [38]

$$\begin{aligned}
m_{\tilde{u}}^2 &= \begin{pmatrix} (m_{\tilde{u}}^2)_{LL} & 0 \\ 0 & (m_{\tilde{u}}^2)_{RR} \end{pmatrix}, \\
m_{\tilde{d}}^2 &= \begin{pmatrix} (m_{\tilde{d}}^2)_{LL} & 0 \\ 0 & (m_{\tilde{d}}^2)_{RR} \end{pmatrix}, \\
m_{\tilde{u}}^{2,\text{diag}} &= Z^U m_{\tilde{u}}^2 (Z^U)^\dagger, \\
m_{\tilde{d}}^{2,\text{diag}} &= Z^D m_{\tilde{d}}^2 (Z^D)^\dagger,
\end{aligned} \tag{7}$$

where

$$\begin{aligned}
(m_{\tilde{u}}^2)_{LL} &= \frac{1}{24}(g_1^2 - 3g_2^2)(v_u^2 - v_d^2) + \frac{1}{3}g_1 v_S M_D^B \\
&\quad + g_2 v_T M_D^W + \frac{1}{2}v_u^2 |Y_u|^2 + m_{\tilde{q}}^2, \\
(m_{\tilde{u}}^2)_{RR} &= \frac{1}{6}g_1^2(v_d^2 - v_u^2) - \frac{4}{3}g_1 v_S M_D^B + \frac{1}{2}v_u^2 |Y_u|^2 + m_{\tilde{u}}^2, \\
(m_{\tilde{d}}^2)_{LL} &= \frac{1}{24}(g_1^2 + 3g_2^2)(v_u^2 - v_d^2) + \frac{1}{3}g_1 v_S M_D^B \\
&\quad - g_2 v_T M_D^W + \frac{1}{2}v_d^2 |Y_d|^2 + m_{\tilde{q}}^2, \\
(m_{\tilde{d}}^2)_{RR} &= \frac{1}{12}g_1^2(v_u^2 - v_d^2) + \frac{2}{3}g_1 v_S M_D^B + \frac{1}{2}v_d^2 |Y_d|^2 + m_{\tilde{d}}^2.
\end{aligned}$$

The explicit expressions of the Feynman rules between fermions, sfermions, and neutralinos/charginos are given as

$$\begin{aligned}
-i\mathcal{L} &= \bar{e}_i [Y_e^i Z_{ki}^{V*} U_{j2}^{1*} P_L - g_2 V_{j1}^1 Z_{ki}^{V*} P_R] \chi_j^\pm \tilde{\nu}_k \\
&\quad + \bar{u}_i [Y_d^i Z_{k(3+i)}^D U_j^1 P_R] \chi_j^\pm \tilde{d}_k \\
&\quad - \bar{e}_i [\sqrt{2} g_1 Z_{k(3+i)}^{E*} N_{j1}^{1*} P_L + Y_e^i N_{j3}^2 Z_{k(3+i)}^{E*} P_R] \chi_j^0 \tilde{e}_k \\
&\quad - \bar{e}_i [Y_e^i N_{j3}^{2*} Z_{ki}^{E*} P_L - \frac{1}{\sqrt{2}} Z_{ki}^{E*} (g_1 N_{j1}^1 + g_2 N_{j2}^1) P_R] \chi_j^{0c} \tilde{e}_k \\
&\quad + \bar{u}_i [\frac{2\sqrt{2}}{3} g_1 N_{j1}^{1*} Z_{k(3+i)}^{U*} P_L - Y_u^i Z_{k(3+i)}^{U*} N_{j4}^2 P_R] \chi_j^0 \tilde{u}_k \\
&\quad - \bar{u}_i [\frac{\sqrt{2}}{6} (3g_2 N_{j2}^{1*} + g_1 N_{j1}^{1*}) Z_{ki}^U P_L + Y_u^i Z_{ki}^U N_{j4}^2 P_R] \chi_j^{0c} \tilde{u}_k \\
&\quad - \bar{d}_i [\frac{2\sqrt{2}}{3} g_1 N_{j1}^{1*} Z_{k(3+i)}^{D*} P_L + Y_d^i Z_{k(3+i)}^{D*} N_{j3}^2 P_R] \chi_j^0 \tilde{d}_k \\
&\quad - \bar{d}_i [Y_d^i N_{j3}^{2*} Z_{ki}^{D*} P_L + \frac{\sqrt{2}}{6} Z_{ki}^{D*} (g_1 N_{j1}^1 - 3g_2 N_{j2}^1) P_R] \chi_j^{0c} \tilde{d}_k \\
&\quad + \bar{d}_i [Y_d^i U_{j2}^{1*} Z_{ki}^{U*} P_L - g_2 Z_{ki}^{U*} V_{j1}^1 P_R] \chi_j^\pm \tilde{u}_k.
\end{aligned} \tag{8}$$

The explicit expressions of the Feynman rules between photon/Z boson and neutralinos/charginos are given as

$$\begin{aligned}
-i\mathcal{L} &= -\bar{\chi}_i^\pm [(2g_2 c_w V_{j1}^{1*} V_{i1}^1 \\
&\quad + \frac{1}{2}(g_2 c_w - g_1 s_w) V_{j2}^{1*} V_{i2}^1) \gamma_\mu P_L + (g_2 c_w U_{i1}^{1*} U_{j2}^1 \\
&\quad + \frac{1}{2}(g_2 c_w - g_1 s_w) U_{i2}^{1*} U_{j2}^1) \gamma_\mu P_R] \chi_j^\pm Z^\mu \\
&\quad + \frac{g_1 s_w + g_2 c_w}{2} \bar{\chi}_i^0 [(N_{j3}^{1*} N_{i3}^1 - N_{j4}^{1*} N_{i4}^1) \gamma_\mu P_L \\
&\quad + (N_{i3}^{2*} N_{j3}^2 - N_{i4}^{2*} N_{j4}^2) \gamma_\mu P_R] \chi_j^0 Z^\mu \\
&\quad - \bar{\chi}_i^\pm [\frac{1}{2}(2g_2 s_w V_{j1}^{1*} V_{i1}^1 + (g_1 c_w + g_2 s_w) V_{j2}^{1*} V_{i2}^1) \gamma_\mu P_L \\
&\quad + \frac{1}{2}(2g_2 s_w U_{i1}^{1*} U_{j1}^1 \\
&\quad + (g_1 c_w + g_2 s_w) U_{i2}^{1*} U_{j2}^1) \gamma_\mu P_R] \chi_j^\pm \epsilon^\mu.
\end{aligned} \tag{9}$$

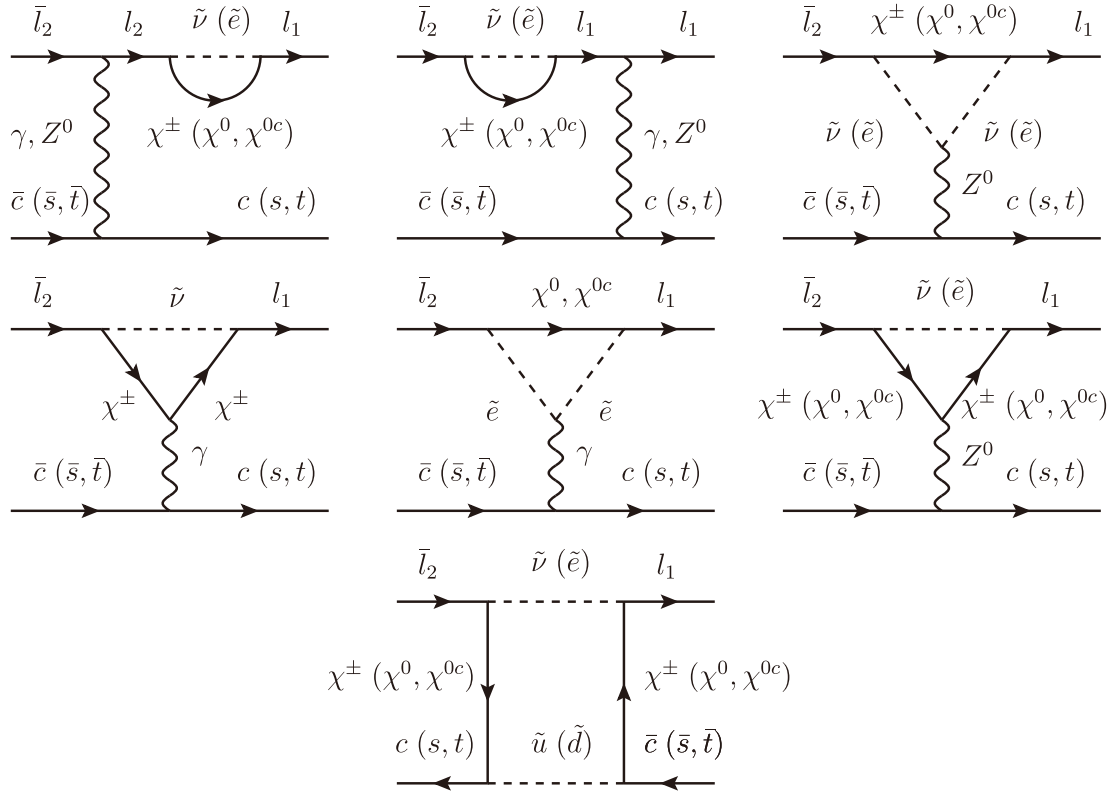
It is noted that the Feynman rules between photon/Z boson and sleptons/sneutrinos are the same as those in the MSSM.

In the following we will discuss the LFV decays $V \rightarrow l_1 l_2$ in detail. The one-loop Feynman diagrams for the LFV decays $V \rightarrow l_1 l_2$ in the MRSSM are shown in Fig. 1. The analytical expression of the BR($V \rightarrow l_1 l_2$) is given in terms of the Wilson coefficients using the effective Lagrangian method in which the general effective Lagrangian for $V \rightarrow l_1 l_2$ is expressed as [19]

$$\begin{aligned}
-\mathcal{L}_{\text{eff}} &= m_2 (C_{DR}^{l_1 l_2} \bar{l}_1 \sigma^{\mu\nu} P_L l_2 + C_{DL}^{l_1 l_2} \bar{l}_1 \sigma^{\mu\nu} P_R l_2) F_{\mu\nu} + \text{h.c.} \\
&\quad + \sum_q [(C_{VR}^{q l_1 l_2} \bar{l}_1 \gamma^\mu P_R l_2 + C_{VL}^{q l_1 l_2} \bar{l}_1 \gamma^\mu P_L l_2) \bar{q} \gamma_\mu q \\
&\quad + (C_{AR}^{q l_1 l_2} \bar{l}_1 \gamma^\mu P_R l_2 + C_{AL}^{q l_1 l_2} \bar{l}_1 \gamma^\mu P_L l_2) \bar{q} \gamma_\mu \gamma_5 q \\
&\quad + m_2 m_q G_F (C_{SR}^{q l_1 l_2} \bar{l}_1 P_L l_2 + C_{SL}^{q l_1 l_2} \bar{l}_1 P_R l_2) \bar{q} q \\
&\quad + m_2 m_q G_F (C_{PR}^{q l_1 l_2} \bar{l}_1 P_L l_2 + C_{PL}^{q l_1 l_2} \bar{l}_1 P_R l_2) \bar{q} \gamma_5 q \\
&\quad + m_2 m_q G_F (C_{TR}^{q l_1 l_2} \bar{l}_1 \sigma^{\mu\nu} P_L l_2 \\
&\quad + C_{TL}^{q l_1 l_2} \bar{l}_1 \sigma^{\mu\nu} P_R l_2) \bar{q} \sigma_{\mu\nu} q + \text{h.c.}],
\end{aligned} \tag{10}$$

where the left/right chiral projection operator $P_{L/R} = \frac{1}{2}(1 \mp \gamma_5)$, G_F stands for the Fermi constant and m_q stands for the mass of the quark q . $C_{DL/DR}^{l_1 l_2}$ in the first row in Eq. (10) are the dipole Wilson coefficients and thus strongly constrained by the radiative decays of the leptons (*i.e.*, $l_1 \rightarrow l_2 \gamma$). The rest are the dimension six four-fermion Lagrangian, where the Wilson coefficients contain the contributions from the Z boson and the Higgs boson excluding the photon.

For the LFV decays $V \rightarrow l_1 l_2$, the general expression of the amplitude is rewritten as [19]


 Fig. 1. The Feynman diagrams for $V \rightarrow l_1 l_2$ in the MRSSM at the one-loop level.

$$\mathcal{A}(V \rightarrow l_1 l_2) = \bar{u}(p_1) \left[A_V^{l_1 l_2} \gamma^\mu + B_V^{l_1 l_2} \gamma^\mu \gamma^5 + \frac{C_V^{l_1 l_2}}{m_V} (p_2 - p_1)_\mu \right. \\ \left. - \frac{D_V^{l_1 l_2}}{m_V} (p_2 - p_1)_\mu \gamma^5 \right] v(p_2) \epsilon^\mu(p), \quad (11)$$

where m_V stands for the mass of the vector meson V , $\epsilon^\mu(p)$ stands for the polarization vector, and p stands for its momentum. The coefficients $A_V^{l_1 l_2}$, $B_V^{l_1 l_2}$, $C_V^{l_1 l_2}$, and $D_V^{l_1 l_2}$ are dimensionless and can be expressed in terms of the Wilson coefficients in Eq. (10) together with the decay constants. The coefficients in Eq. (11) are derived as [19]

$$A_V^{l_1 l_2} = \sqrt{4\pi\alpha} Q_q y^2 (C_{DL}^{l_1 l_2} + C_{DR}^{l_1 l_2}) + \kappa_V (C_{VL}^{q l_1 l_2} + C_{VR}^{q l_1 l_2}) \\ + 2y^2 \kappa_V \frac{f_V^T}{f_V} G_F m_V m_q (C_{TL}^{q l_1 l_2} + C_{TR}^{q l_1 l_2}), \\ B_V^{l_1 l_2} = -\sqrt{4\pi\alpha} Q_q y^2 (C_{DL}^{l_1 l_2} - C_{DR}^{l_1 l_2}) - \kappa_V (C_{VL}^{q l_1 l_2} - C_{VR}^{q l_1 l_2}) \\ - 2y^2 \kappa_V \frac{f_V^T}{f_V} G_F m_V m_q (C_{TL}^{q l_1 l_2} - C_{TR}^{q l_1 l_2}), \\ C_V^{l_1 l_2} = \sqrt{4\pi\alpha} Q_q y (C_{DL}^{l_1 l_2} + C_{DR}^{l_1 l_2}) \\ + 2\kappa_V \frac{f_V^T}{f_V} G_F m_2 m_q (C_{TL}^{q l_1 l_2} + C_{TR}^{q l_1 l_2}),$$

$$D_V^{l_1 l_2} = -\sqrt{4\pi\alpha} Q_q y (C_{DL}^{l_1 l_2} - C_{DR}^{l_1 l_2}) \\ + 2\kappa_V \frac{f_V^T}{f_V} G_F m_2 m_q (C_{TL}^{q l_1 l_2} - C_{TR}^{q l_1 l_2}), \quad (12)$$

where α stands for the fine structure constant, Q_q stands for the charge of the quark q , $y = \frac{m_2}{m_V}$, and $\kappa_V = \frac{1}{2}$ for the pure $q\bar{q}$ states. It is noted that, different from the definition of $D_V^{l_1 l_2}$ in [19], the imaginary unit was not considered in this work. From Eq. (12) we see that the contributions of the Higgs mediated self-energies and penguin diagrams are nonexistent since these diagrams only contribute to the Wilson coefficients corresponding to the scalar and the pseudo-scalar operators in Eq. (10). The contributions of the tensor operators can be neglected in the MRSSM since the coefficients $C_{TL/TR}^{q l_1 l_2}$ (corresponding to the Feynman diagrams in Fig. 1) are computed as zero. The definitions of the decay constant f_V and the transverse decay constant f_V^T are

$$\langle 0 | \bar{q} \gamma^\mu q | V(p) \rangle = f_V m_V \epsilon^\mu(p), \\ \langle 0 | \bar{q} \sigma^{\mu\nu} q | V(p) \rangle = i f_V^T (\epsilon^\mu p^\nu - \epsilon^\nu p^\mu). \quad (13)$$

In the following, we list the general expressions of the Wilson coefficients, where F, S denote the fermion and the scalar particle, respectively. The coefficients $C_{VL}^{l_1 l_2}$ for

the self-energy diagrams in Fig. 1 are

$$C_{VL}^{ql_1l_2} = \frac{C_L^{l_1l_2Z}}{(m_{l_1}^2 - m_{l_2}^2)m_Z^2} (C_L^{qqZ} + C_R^{qqZ})$$

$$\times (m_{l_1}^2 C_L^{FSl_1} C_R^{FSl_2*} B_1(0, m_F^2, m_S^2)$$

$$- m_{l_1} m_F C_R^{FSl_1} C_L^{FSl_2*} B_0(0, m_F^2, m_S^2)$$

$$+ m_{l_1} m_{l_2} C_R^{FSl_1} C_L^{FSl_2*} B_1(0, m_F^2, m_S^2)$$

$$- m_{l_2} m_F C_L^{FSl_1} C_R^{FSl_2*} B_0(0, m_F^2, m_S^2)),$$

$$C_{VL}^{ql_1l_2} = \frac{C_L^{l_1l_1Z}}{(m_{l_1}^2 - m_{l_2}^2)m_Z^2} (C_L^{qqZ} + C_R^{qqZ})$$

$$\times (m_{l_2}^2 C_R^{FSl_2*} C_L^{FSl_1} B_1(0, m_F^2, m_S^2)$$

$$- m_{l_2} m_F C_L^{FSl_2*} C_R^{FSl_1} B_0(0, m_F^2, m_S^2)$$

$$+ m_{l_2} m_{l_1} C_L^{FSl_2*} C_R^{FSl_1} B_1(0, m_F^2, m_S^2)$$

$$- m_{l_1} m_F C_R^{FSl_2*} C_L^{FSl_1} B_0(0, m_F^2, m_S^2)),$$

with $FS \in \{\chi^0 \tilde{e}, \chi^{0c} \tilde{e}, \chi^\pm \tilde{\nu}\}$. $q \in \{c, s, b\}$ depends on the components of the vector mesons. $C_{L/R}^{qqZ}, C_{L/R}^{FSl_1}, \dots$, stand for the interaction of q - q - Z, F - S - l_1 , *etc.* The coefficients $C_{VL}^{l_1l_2}$ for the triangle diagrams in Fig. 1 are

$$C_{VL}^{ql_1l_2} = -\frac{2}{m_Z^2} C_L^{FSl_1l_1} C_R^{FSl_2l_2*} C^{S_1S_2Z} (C_L^{qqZ} + C_R^{qqZ})$$

$$\times C'_{00}(m_F^2, m_{S_2}^2, m_{S_1}^2),$$

$$C_{VL}^{ql_1l_2} = \frac{1}{m_Z^2} C_L^{F_1S_1l_1} C_R^{F_2S_2l_2*} (C_R^{F_1F_2Z} (B'_0(m_{F_2}^2, m_{F_1}^2, m_S^2)$$

$$- 2C'_{00}(m_{F_2}^2, m_{F_1}^2, m_S^2))$$

$$- C_L^{F_1F_2Z} C'_0(m_{F_2}^2, m_{F_1}^2, m_S^2) m_{F_1} m_{F_2}) (C_L^{qqZ} + C_R^{qqZ}),$$

with $FS_1S_2 \in \{\chi^\pm \tilde{\nu} \tilde{\nu}, \chi^0 \tilde{e} \tilde{e}, \chi^{0c} \tilde{e} \tilde{e}\}$ and $F_1F_2S \in \{\chi^0 \chi^0 \tilde{e}, \chi^{0c} \chi^{0c} \tilde{e}, \chi^\pm \chi^\pm \tilde{\nu}\}$. The coefficients $C_{DL}^{l_1l_2}$ for the triangle diagrams in Fig. 1 are

$$C_{DL}^{ql_1l_2} = \frac{C^{S_1S_2\gamma}}{\sqrt{4\pi\alpha_Z}} (m_{l_1} C_R^{FS_1l_1*} C_L^{FS_2l_2} C'_2(m_{F_2}^2, m_{S_2}^2, m_{S_1}^2)$$

$$+ m_{l_2} C_L^{FS_1l_1*} C_R^{FS_2l_2}$$

$$\times C'_1(m_{F_2}^2, m_{S_2}^2, m_{S_1}^2) - m_F C_L^{FS_1l_1*} C_L^{FS_2l_2} C'_0(m_{F_2}^2, m_{S_2}^2, m_{S_1}^2))$$

$$C_{DL}^{ql_1l_2} = \frac{1}{\sqrt{4\pi\alpha_Z}} (m_{l_1} C_R^{F_1S_1l_1*} C_L^{F_2S_2l_2} C_L^{F_1F_2\gamma} C'_{12}(m_{F_2}^2, m_{F_1}^2, m_S^2)$$

$$- m_{l_2} C_L^{F_1S_1l_1*} C_R^{F_2S_2l_2}$$

$$\times C_R^{F_1F_2\gamma} C'_2(m_{F_2}^2, m_{F_1}^2, m_S^2)$$

$$- m_{F_1} C_R^{F_1S_1l_1*} C_L^{F_2S_2l_2} C_L^{F_1F_2\gamma} C'_1(m_{F_2}^2, m_{F_1}^2, m_S^2)$$

$$+ m_{F_2} C_L^{F_1S_1l_1*} C_R^{F_2S_2l_2} C_R^{F_1F_2\gamma} C'_0(m_{F_2}^2, m_{F_1}^2, m_S^2)),$$

with $FS_1S_2 \in \{\chi^\pm \tilde{\nu} \tilde{\nu}, \chi^0 \tilde{e} \tilde{e}, \chi^{0c} \tilde{e} \tilde{e}\}$ and $F_1F_2S \in \{\chi^0 \chi^0 \tilde{e}, \chi^{0c} \chi^{0c} \tilde{e}, \chi^\pm \chi^\pm \tilde{\nu}\}$. The coefficients $C_{VL}^{l_1l_2}$ for the box diagrams in Fig. 1 are

$$C_{VL}^{ql_1l_2} = C_L^{F_1S_1l_1} C_R^{F_2S_2l_2*} (\frac{1}{2} C_R^{F_1S_2q} C_L^{F_2S_2q*} D'_0$$

$$\times (m_{F_1}, m_{F_2}, m_{F_2}^2, m_{F_1}^2, m_{S_1}^2, m_{S_2}^2)$$

$$- C_L^{F_1S_2q} C_R^{F_2S_2q*} D'_{00}(m_{F_2}^2, m_{F_1}^2, m_{S_1}^2, m_{S_2}^2)),$$

with $F_1F_2S_1S_2 \in \{\chi^\pm \chi^\pm \tilde{\nu} \tilde{\nu}(\tilde{u}), \chi^0 \chi^0 \tilde{e} \tilde{e}(\tilde{d}), \chi^{0c} \chi^{0c} \tilde{e} \tilde{e}(\tilde{d}), \chi^0 \chi^{0c} \tilde{e} \tilde{e}(\tilde{d}), \chi^{0c} \chi^{0c} \tilde{e} \tilde{e}(\tilde{d})\}$. The coefficients are left-right symmetric, *i.e.*, $C_{VR}^{ql_1l_2} = C_{VL}^{ql_1l_2} (L \leftrightarrow R)$ and $C_{DR}^{ql_1l_2} = C_{DL}^{ql_1l_2} (L \leftrightarrow R)$. The explicit expressions of the loop integrals are given elsewhere [57–60]. The expressions of the Wilson coefficients in the MRSSM were added to the Mathematica package SARAH [59–63] to generate modules for the Fortran package SPheno [57, 58].

The amplitude in Eq. (11) leads to the branching ratio $\text{BR}(V \rightarrow l_1 l_2)$, which is conveniently given as [19]

$$\text{BR}(V \rightarrow l_1 l_2) = \text{BR}(V \rightarrow ee) \times \left(\frac{m_V^2 (1 - y^2)^2}{4\pi\alpha Q_q} \right)^2$$

$$\times \left[|A_V^{l_1l_2}|^2 + |B_V^{l_1l_2}|^2 \right.$$

$$+ \left(\frac{1}{2} - 2y^2 \right) (|C_V^{l_1l_2}|^2 + |D_V^{l_1l_2}|^2)$$

$$\left. + y \text{Re}(A_V^{l_1l_2} C_V^{l_1l_2*} + B_V^{l_1l_2} D_V^{l_1l_2*}) \right], \quad (14)$$

where the mass of the lighter one of the two final leptons is set to zero.

III. NUMERICAL ANALYSIS

In Table 3, we provide a list of values of the vector masses, the decay constants and $\text{BR}(V \rightarrow ee)$ used for calculating $\text{BR}(V \rightarrow l_1 l_2)$; all the mass parameters are in GeV [19, 64]. Following the suggestion in Ref. [65] and the fact that the branching ratio in Eq. (14) is, to a large extent, independent of the value of the decay constant [19], the transverse decay constants of the vectors are the same (*i.e.*, $f_V^T = f_V$) except for J/ψ , which is $f_{J/\psi}^T = 0.410$ GeV.

The most accurate prediction for the mass of the SM-like Higgs boson as well as the W boson in the MRSSM was given in Ref. [43], with the following set of benchmark points:

$$\mu_u = \mu_d = 500, M_D^W = 600, M_D^B = 550, \Lambda_d = -1.2, \lambda_d = 1.0,$$

$$\Lambda_u = -1.1, \lambda_u = -0.8, B_\mu = 500^2, v_S = 5.9, \tan\beta = 3,$$

$$(m_i^2)_{ii} = (m_r^2)_{ii} = 1000^2 \quad (i = 1, 2, 3), v_T = -0.38,$$

Table 3. Values used in the calculation.

Vector	ϕ	J/ψ	$\psi(2S)$	$\Upsilon(1S)$	$\Upsilon(2S)$	$\Upsilon(3S)$
m_V	1.0194	3.0969	3.686	9.4603	10.023	10.355
f_V	0.241	0.418	0.294	0.649	0.481	0.539
$BR(V \rightarrow ee)$	2.973×10^{-4}	5.971×10^{-2}	7.93×10^{-3}	2.38×10^{-2}	1.91×10^{-2}	2.18×10^{-2}

$$(m_{\tilde{q}}^2)_{ii} = (m_{\tilde{u}}^2)_{ii} = (m_{\tilde{d}}^2)_{ii} = 2500^2 \quad (i = 1, 2), m_T = 3000,$$

$$(m_{\tilde{q}}^2)_{ii} = (m_{\tilde{u}}^2)_{ii} = (m_{\tilde{d}}^2)_{ii} = 1000^2 \quad (i = 3), m_S = 2000, \quad (15)$$

where the mass parameters are in GeV or GeV². The predicted W boson mass in the MRSSM is comparable with the result from the combined Large Electron-Positron (LEP) collider and Fermilab Tevatron collider measurements [66], the result from the ATLAS collaboration [67] and the result from the LHCb Collaboration [68], which is more precise than the LEP result. By changing the values of some parameters, e.g. m_{SUSY} , v_T , Λ_u and Λ_d , the recent result for the W boson mass obtained by the CDF collaboration [69] can also be accommodated in the MRSSM [43, 53]. It is noted that these parameters have very little effect on the predicted $BR(V \rightarrow l_1 l_2)$, which takes values within a narrow range. The default values of the input parameters are given in Eq. (15) in the following analysis. Note that the off-diagonal inputs of the slepton mass matrices m_l^2 , m_r^2 as well as the squark mass matrices $m_{\tilde{q}}^2$, $m_{\tilde{u}}^2$, $m_{\tilde{d}}^2$ in Eq. (15) are zero.

The LFV decays arise from the off-diagonal inputs of the 3×3 slepton mass matrices m_l^2 and m_r^2 . These off-diagonal inputs of matrices m_l^2 and m_r^2 are usually parameterized by the mass insertions

$$(m_l^2)^{IJ} = \delta_l^{IJ} \sqrt{(m_l^2)^{II} (m_l^2)^{JJ}},$$

$$(m_r^2)^{IJ} = \delta_r^{IJ} \sqrt{(m_r^2)^{II} (m_r^2)^{JJ}}, \quad (I, J = 1, 2, 3).$$

Before the numerical computation, some assumptions were made to decrease the number of free parameters. The parameters δ_l^{IJ} and δ_r^{IJ} were strongly constrained by the experimental limitations on several LFV decays, for example, the radiative two body decays ($l_2 \rightarrow l_1 \gamma$), the leptonic three body decays ($l_2 \rightarrow 3l_1$), and $\mu - e$ conversions in nuclei. We list the current limits of the above LFV decays in Table 4 [64]. Both δ_l^{IJ} and δ_r^{IJ} have a perceptible effect on the prediction of the branching ratio of the lepton flavor violating processes, with δ_l^{IJ} having a

stronger effect than δ_r^{IJ} . For simplicity and for obtaining larger predictions of the branching ratios, we assumed $\delta_l^{IJ} = \delta_r^{IJ} = \delta^{IJ}$ and then $\delta^{IJ} = \delta^{12}$, δ^{13} or δ^{23} . In the following we used the experimental limits in Table 4 to constrain the parameters δ^{IJ} .

We give the corresponding predictions for $BR(V \rightarrow l_1 l_2)$ in Fig. 2 along with the other SUSY parameters in Eq. (15) where the predictions for $BR(l_1 \rightarrow l_2 \gamma)$, $BR(l_1 \rightarrow 3l_2)$ and $CR(\mu - e, Ti)$ are also presented. Results are shown as functions of one of the parameters δ^{IJ} . In all plots, only the indicated δ^{IJ} is varied with all other mass insertions set to zero. The predictions for $BR(\Upsilon(nS) \rightarrow l_1 l_2)$ in each plot are very close to each other. The predictions for $BR(V \rightarrow e^- \mu^+)$, $BR(V \rightarrow e^- \tau^+)$, and $BR(V \rightarrow \mu^- \tau^+)$ were affected by the mass insertions δ^{12} , δ^{13} , and δ^{23} , respectively. The predicted $BR(V \rightarrow l_1 l_2)$ in the MRSSM was below 10^{-14} and was at least seven orders of magnitude below the current experimental limit. A linear relationship was obtained between the branching ratios and the flavor violating parameters δ^{IJ} owing to the fact that both x axis and y axis in Fig. 2 were logarithmically scaled. The actual dependence on δ^{IJ} was quadratic. The following hierarchy is shown in Fig. 2, $BR(\Upsilon(3S) \rightarrow l_1 l_2) > BR(\Upsilon(2S) \rightarrow l_1 l_2) \sim BR(\Upsilon(1S) \rightarrow l_1 l_2) > BR(J/\psi \rightarrow l_1 l_2) > BR(\psi(2S) \rightarrow l_1 l_2) > BR(\phi \rightarrow l_1 l_2)$. The same hierarchy appeared in several new physics scenarios [1, 14]. The most challenging experimental prospects for δ^{12} arose for $\mu \rightarrow e \gamma$. Considering that the new sensitivity for $BR(\mu \rightarrow e \gamma)$ will be approximately 6×10^{-14} in the future projects of MEG II [70], δ^{12} was constrained to be approximately 10^{-3} . The constraints on δ^{13} from $\tau \rightarrow e \gamma$ and $\tau \rightarrow 3e$ were comparable, and δ^{13} was constrained to be approximately $10^{-0.2}$. The case for δ^{23} was the same as that for δ^{13} .

In the following, we consider the process $\Upsilon(3S) \rightarrow l_1 l_2$ as an example since the behavior for $\Upsilon(3S)$ also exists for ϕ , J/ψ , $\psi(2S)$, $\Upsilon(1S)$, and $\Upsilon(2S)$. We present the corresponding predictions for $BR(\Upsilon(3S) \rightarrow l_1 l_2)$ from various parts as functions of $\tan\beta$ in Fig. 3, where $\delta^{12} = 10^{-3} (e\mu)$, $\delta^{13} = 10^{-0.2} (e\tau)$, and $\delta^{23} = 10^{-0.2} (\mu\tau)$ are

Table 4. Current limits on the $l_1 \rightarrow l_2 \gamma$, $l_1 \rightarrow 3l_2$ and $\mu - e$ conversions for Ti targets.

Decay	Limit	Decay	Limit	Decay	Limit	Decay	Limit
$\mu \rightarrow e \gamma$	4.2×10^{-13}	$\mu \rightarrow 3e$	1.0×10^{-12}	$\tau \rightarrow e \gamma$	3.3×10^{-8}	$\tau \rightarrow 3e$	2.7×10^{-8}
$\tau \rightarrow \mu \gamma$	4.4×10^{-8}	$\tau \rightarrow 3\mu$	2.1×10^{-8}	$\mu - e, Ti$	4.3×10^{-12}		

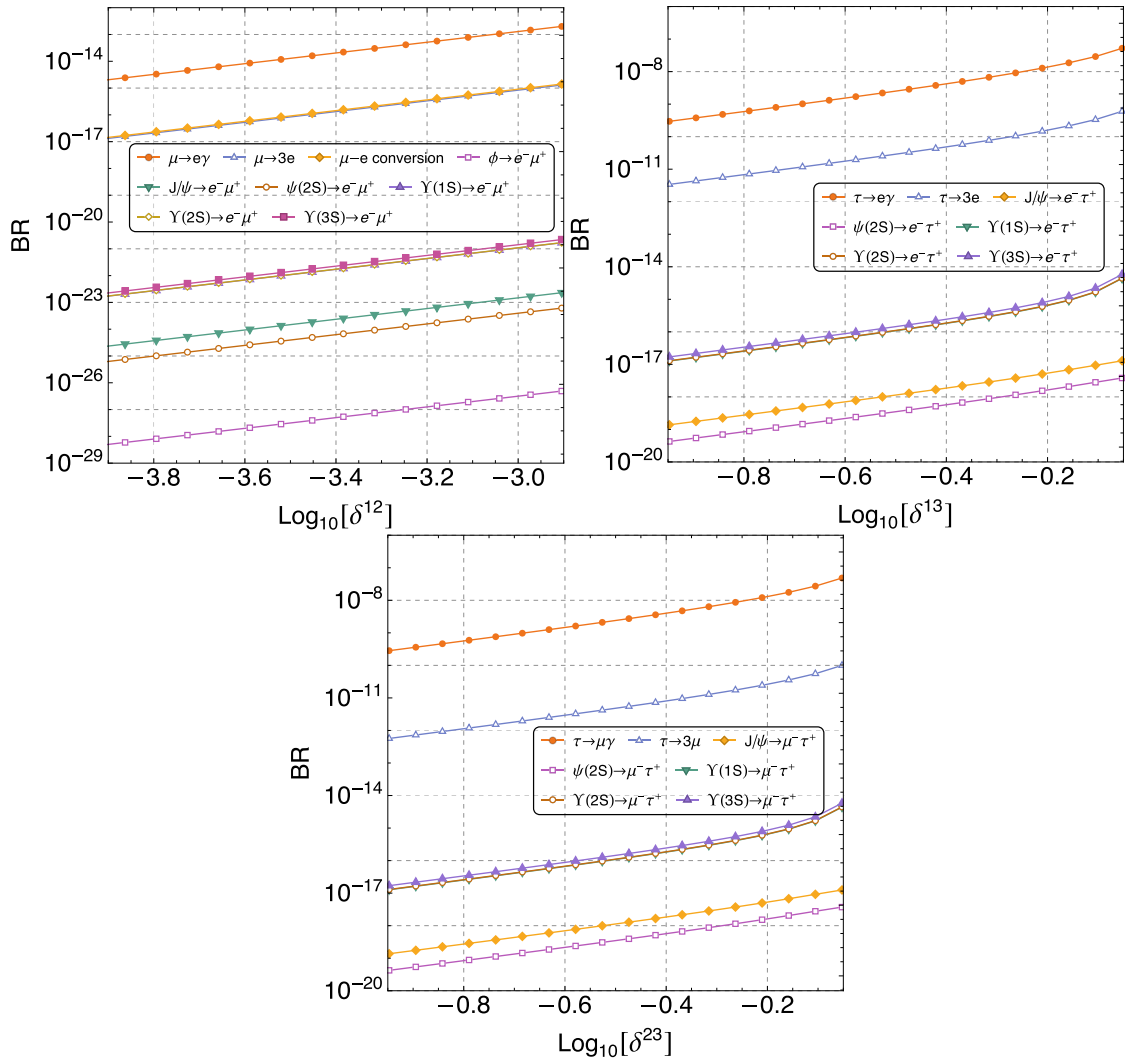


Fig. 2. (color online) Predictions for $\text{BR}(V \rightarrow l_1 l_2)$ in the MRSSM. Note that the predictions for $\text{BR}(\Upsilon(nS) \rightarrow l_1 l_2)$ in each plot are very close to each other.

used. The lines corresponding to "Z," " γ ," and "Box" stand for the values of $\text{BR}(\Upsilon(3S) \rightarrow l_1 l_2)$ obtained by only considering the listed contribution without any others. The predicted $\text{BR}(\Upsilon(3S) \rightarrow l_1 l_2)$ with the total contribution is also indicated. We observe that the contributions from different parts are comparable, and the following order holds: $\text{BR}(\Upsilon(3S) \rightarrow l_1 l_2, Z) > \text{BR}(\Upsilon(3S) \rightarrow l_1 l_2, \text{Total}) > \text{BR}(\Upsilon(3S) \rightarrow l_1 l_2, \gamma) > \text{BR}(J/\psi \rightarrow l_1 l_2, \text{Box})$ (for J/ψ , $\psi(2S)$, $\text{BR}(\Upsilon(3S) \rightarrow l_1 l_2, \gamma) > \text{BR}(\Upsilon(3S) \rightarrow l_1 l_2, \text{Total})$). For small values of $\tan\beta$, the prediction for Z penguin changes quickly, since the branching ratios are proportional to the reciprocal of $\tan\beta^2$, and for the same reason, the prediction for Z penguin changes slowly for higher values of $\tan\beta$. This behavior is also observed for the $\mu-e$ conversion [38, 71] and for the $\tau \rightarrow Pl$ process [55], both of which gain the contribution from the similar Z penguin diagrams excluding the quark sector.

We present the contour plots of $\text{BR}(\Upsilon(3S) \rightarrow l_1 l_2)$ in

the $mQ \sim mL$ plane in Fig. 4, where $mQ = \sqrt{(m_{\tilde{q}}^2)_{ii}} = \sqrt{(m_{\tilde{u}}^2)_{ii}} = \sqrt{(m_{\tilde{d}}^2)_{ii}}$ ($i = 1, 2, 3$) and $mL = \sqrt{(m_l^2)_{ii}} = \sqrt{(m_{\tau}^2)_{ii}}$ ($i = 1, 2, 3$) are assumed. The predictions for $\text{BR}(\Upsilon(3S) \rightarrow l_1 l_2)$ are sensitive to mQ and mL . The predictions for $\text{BR}(\Upsilon(3S) \rightarrow l_1 l_2)$ increase slowly when the parameter mQ varies from 1 TeV to 5 TeV and decrease slowly when the parameter mL varies from 1 TeV to 5 TeV. For a wide range of mQ and mL values, the predictions for $\text{BR}(\Upsilon(3S) \rightarrow l_1 l_2)$ change by approximately one order of magnitude. The off-diagonal inputs $\delta_{\tilde{q}, \tilde{u}, \tilde{d}}^{IJ}$ of the mass matrices $m_{\tilde{q}}^2$, $m_{\tilde{u}}^2$ and $m_{\tilde{d}}^2$ have very little effect on the predicted $\text{BR}(\Upsilon(3S) \rightarrow l_1 l_2)$, which takes values in a narrow range. The effect from the off-diagonal inputs of the squark mass matrices is too small to be neglected. It is noted that the effects of the other parameters in Eq. (15) are the same as those described in Refs. [55, 56].

The final results on the upper bounds of $\text{BR}(V \rightarrow l_1 l_2)$

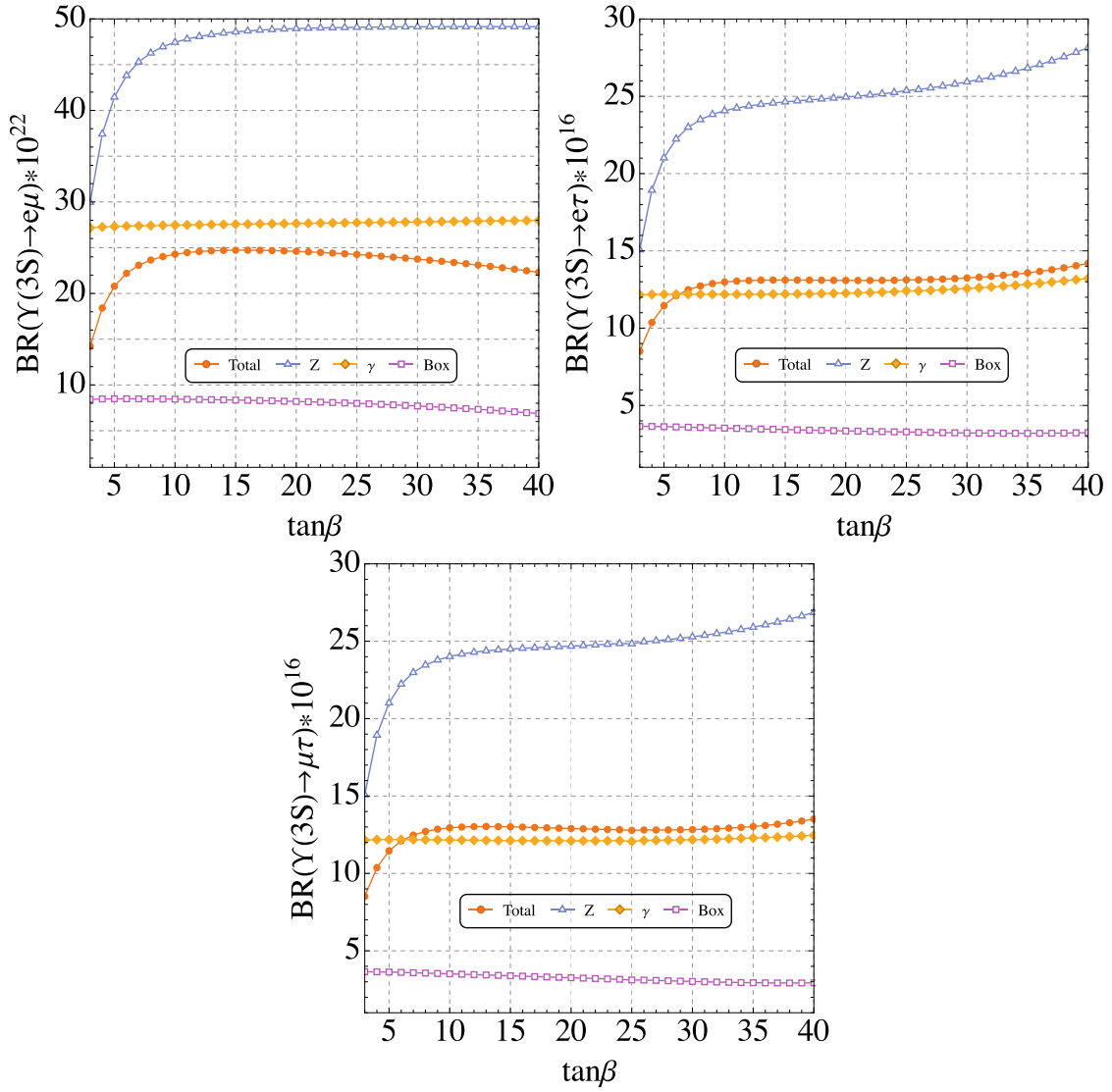


Fig. 3. (color online) Contributions to $\text{BR}(\Upsilon(3S) \rightarrow l_1 l_2)$ from various parts in the MRSSM.

in the MRSSM are given in Table 5; those were obtained by assuming $\delta^{12}=10^{-3}$, $\delta^{13}=10^{-0.2} (\approx 0.63)$ and $\delta^{23}=10^{-0.2}$, respectively, and the results in the literature are also included for comparison. Using an effective field theory, the data in Ref. [20] were obtained from the recast of high- p_T dilepton tails at the LHC for the left-handed scenario, where dipole operators were not considered. The expressions for $\text{BR}(V \rightarrow l_1 l_2)$ in Ref. [20] were the same, except for a few adjustments (e.g., mass, decay constant and full width). Since the mass, decay constant and full width for $\psi(2S)$ are very close to J/ψ , the bounds for $\psi(2S) \rightarrow l_1 l_2$ were on the same level as $J/\psi \rightarrow l_1 l_2$. For the same reason, the bounds for $\Upsilon(1S) \rightarrow l_1 l_2$ and $\Upsilon(2S) \rightarrow l_1 l_2$ were on the same level as $\Upsilon(3S) \rightarrow l_1 l_2$. The predicted values for $\text{BR}(V \rightarrow l\tau)$ in the MRSSM ranged between the values reported in Ref. [1] and Ref. [14], and the predicted values for $\text{BR}(V \rightarrow e\mu)$ were below those reported in Ref. [1] and Ref. [14]. All the direct bounds in

new physics scenarios were smaller than the indirect bounds in Ref. [20]. The limits on $\text{BR}(V \rightarrow l_1 l_2)$ in the MRSSM were more than ten orders of magnitude smaller than the current limits or future experimental sensitivities [24, 27, 29, 72].

IV. CONCLUSIONS

Although higher order LFV processes in the SM are permitted, these are extremely suppressed by the powers of small neutrino masses, making it impossible to obtain LFV signals in current and future experiments. From this point of view, observations of the LFV decays could indicate new physics, beyond the SM.

In this study, we analyzed the LFV decays of vector mesons $V \rightarrow l_1 l_2$ in the framework of the MRSSM, accounting for the constraints on the mass insertion parameters δ^{ij} from the radiative charged lepton decays

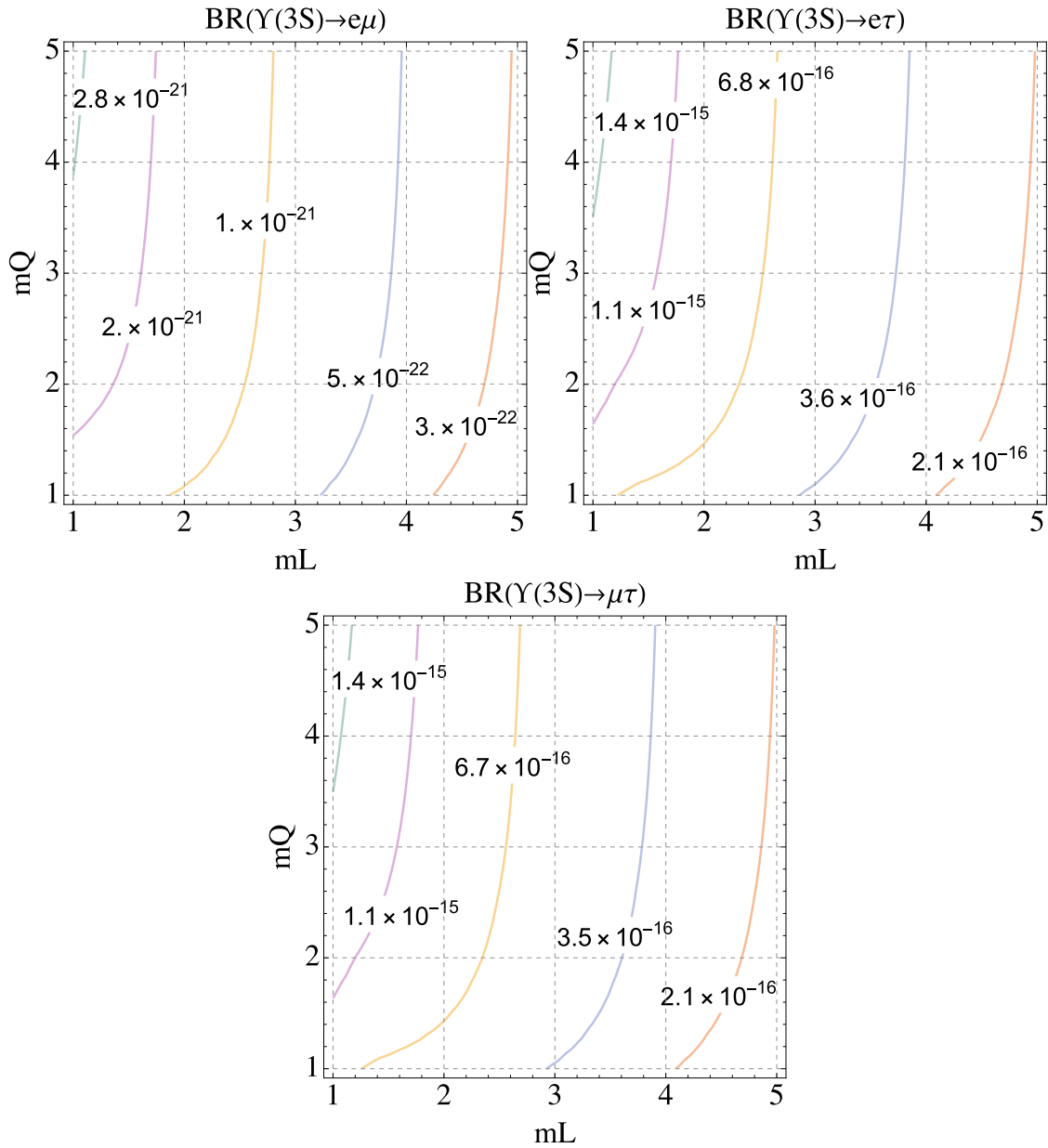


Fig. 4. (color online) Contour plots showing the behavior of $\text{BR}(\Upsilon(3S) \rightarrow l_1 l_2)$ as a function of mQ and mL .

$(l_1 \rightarrow l_2 \gamma)$, leptonic three body decays ($l_1 \rightarrow 3l_2$), and μ - e conversion in nuclei. The predictions for $\text{BR}(V \rightarrow e^- \mu^+)$, $\text{BR}(V \rightarrow e^- \tau^+)$, and $\text{BR}(V \rightarrow \mu^- \tau^+)$ were dominated by the mass insertions δ^{12} , δ^{13} , and δ^{23} , respectively. It is thought that the LFV decays of mesons may be significantly enhanced by the off-diagonal inputs $\delta_{\tilde{q}, \tilde{u}, \tilde{d}}^{IJ}$. However, as far as we know, this depends on the structure of mesons. The enhancement would be large for the mesons containing two different generation quarks and small for those containing two same generation quarks. For the vector mesons J/ψ , $\Upsilon(nS)$, and ϕ , the effect from the off-diagonal inputs of the squark mass matrices would be too small to be neglected. The final results for the upper bounds of $\text{BR}(V \rightarrow l_1 l_2)$ in the MRSSM are given in

Table 5 and were obtained by assuming $\delta^{12} = 10^{-3}$, $\delta^{13} = 10^{-0.2}$, and $\delta^{23} = 10^{-0.2}$, respectively. Literature results were also included for comparison. The predictions for $\text{BR}(V \rightarrow l_1 l_2)$ in the MRSSM were much smaller than the current upper limits.

The studies of the radiative LFV (RLFV) decays of vector mesons $V \rightarrow \gamma l_1 l_2$ showed that the RLFV decays might be a new way to search for new physics [19]. Besides the dipole, vector, and tensor operators, the RLFV decays $V \rightarrow \gamma l_1 l_2$ could receive contributions through the axial, scalar, and pseudoscalar operators, which are not accessible in the Feynman diagrams of $V \rightarrow l_1 l_2$, *e.g.*, the Higgs mediated self-energies and penguin diagrams. If only considering the contribution from the scalar operat-

Table 5. The upper limits on $\text{BR}(V \rightarrow l_1 l_2)$ in literature and in the MRSSM.

Decay	Ref. [20](3 ab ⁻¹)	Ref. [1]((2,3)-ISS)	Ref. [14](331)	this work (MRSSM)
$\phi \rightarrow e\mu$	1.2×10^{-18}	1×10^{-23}	8.1×10^{-23}	3.2×10^{-27}
$J/\psi \rightarrow e\mu$	1.6×10^{-12}	2×10^{-20}	7.7×10^{-20}	1.5×10^{-23}
$J/\psi \rightarrow e\tau$	4.8×10^{-12}	1×10^{-19}	6.3×10^{-15}	5.3×10^{-18}
$J/\psi \rightarrow \mu\tau$	6.4×10^{-12}	4×10^{-19}	5.2×10^{-15}	5.3×10^{-18}
$\psi(2S) \rightarrow e\mu$	-	4×10^{-21}	2.1×10^{-20}	3.9×10^{-24}
$\psi(2S) \rightarrow e\tau$	-	4×10^{-20}	2.1×10^{-15}	1.6×10^{-18}
$\psi(2S) \rightarrow \mu\tau$	-	1×10^{-19}	1.7×10^{-15}	1.6×10^{-18}
$\Upsilon(1S) \rightarrow e\mu$	-	2×10^{-19}	3.8×10^{-17}	1.0×10^{-21}
$\Upsilon(1S) \rightarrow e\tau$	-	6×10^{-18}	5.5×10^{-12}	6.4×10^{-16}
$\Upsilon(1S) \rightarrow \mu\tau$	-	1×10^{-17}	4.3×10^{-12}	6.4×10^{-16}
$\Upsilon(2S) \rightarrow e\mu$	-	2×10^{-19}	4.2×10^{-17}	1.1×10^{-21}
$\Upsilon(2S) \rightarrow e\tau$	-	8×10^{-18}	6.1×10^{-12}	6.5×10^{-16}
$\Upsilon(2S) \rightarrow \mu\tau$	-	2×10^{-17}	4.8×10^{-12}	6.5×10^{-16}
$\Upsilon(3S) \rightarrow e\mu$	1.3×10^{-9}	5×10^{-19}	9.1×10^{-17}	1.4×10^{-21}
$\Upsilon(3S) \rightarrow e\tau$	7.9×10^{-9}	2×10^{-17}	1.3×10^{-11}	8.5×10^{-16}
$\Upsilon(3S) \rightarrow \mu\tau$	1.2×10^{-8}	3×10^{-17}	1.0×10^{-11}	8.5×10^{-16}

ors [22], the indirect upper limits on $\text{BR}(\Upsilon(1S) \rightarrow \gamma l_1 \tau)$ could be approximately two to three orders of magnitude smaller than the current result from the Belle collaboration [27]. It might be possible that the RLFV processes

$V \rightarrow \gamma l_1 l_2$ could be enhanced close to the sensitivities of the current or planned experiment, while the LFV decays $V \rightarrow l_1 l_2$ remain out of the reach of current experiments.

References

- [1] A. Abada, D. Beirevi, M. Lucente *et al.*, *Phys. Rev. D* **91**, 113013 (2015)
- [2] P. Langacker, *Phys. Rep.* **72**, 185 (1981)
- [3] H. Georgi and S. L. Glashow, *Phys. Rev. Lett.* **32**, 438 (1974)
- [4] J. C. Pati and A. Salam, *Phys. Rev. D* **10**, 275 (1974)
- [5] G. C. Branco, P. M. Ferreira, L. Lavoura *et al.*, *Phys. Rept.* **516**, 1-102 (2012)
- [6] H. E. Haber and G. L. Kane, *Phys. Rep.* **117**, 75 (1985)
- [7] G. Senjanovic and R. N. Mohapatra, *Phys. Rev. D* **12**, 1502 (1975)
- [8] R. N. Mohapatra and J. C. Pati, *Phys. Rev. D* **11**, 2558 (1975)
- [9] R. N. Mohapatra and J. C. Pati, *Phys. Rev. D* **11**, 566 (1975)
- [10] Z.-T. Wei, Y. Xu, and X.-Q. Li, *Eur. Phys. J. C* **62**, 593 (2009)
- [11] W.-J. Huo, T.-F. Feng, and C.-X. Yue, *Phys. Rev. D* **67**, 114001 (2003)
- [12] K.-S. Sun, T.-F. Feng, T.-J. Gao *et al.*, *Nucl. Phys. B* **865**, 486 (2012)
- [13] K.-S. Sun, T.-F. Feng, L.-N. Kou *et al.*, *Mod. Phys. Lett. A* **27**, 1250172 (2012)
- [14] C.-X. Yue and J.-R. Zhou, *Phys. Rev. D* **93**, 035021 (2016)
- [15] X.-X. Dong, S.-M. Zhao, J.-J. Feng *et al.*, *Phys. Rev. D* **97**, 056027 (2018)
- [16] S. Nussinov, R. D. Peccei, and X. M. Zhang, *Phys. Rev. D* **63**, 016003 (2001)
- [17] T. Gutsche, J. C. Helo, S. Kovalenko *et al.*, *Phys. Rev. D* **81**, 037702 (2010)
- [18] T. Gutsche, J. C. Helo, S. Kovalenko *et al.*, *Phys. Rev. D* **83**, 115015 (2011)
- [19] D. E. Hazard and A. A. Petrov, *Phys. Rev. D* **94**, 074023 (2016)
- [20] A. Angelescu, D. A. Faroughy, and O. Sumensari, *Eur. Phys. J. C* **80**, 641 (2020)
- [21] M. Gonzalez, S. Kovalenko, and J. Vignatti, *Eur. Phys. J. C* **82**, 312 (2022)
- [22] L. Calibbi, T. Li, X. Marcano *et al.*, *Phys. Rev. D* **106**, 115039 (2022)
- [23] M. Ablikim *et al.* (BESIII Collaboration), *Sci. China Phys. Mech. Astron.* **66**, 221011 (2023)
- [24] M. Ablikim *et al.* (BESIII Collaboration), *Phys. Rev. D* **103**, 112007 (2021)
- [25] M. Ablikim *et al.* (BESIII Collaboration), *Phys. Rev. D* **87**, 112007 (2013)
- [26] M. Ablikim *et al.* (BES Collaboration), *Phys. Lett. B* **598**, 172 (2004)
- [27] S. Patra *et al.* (Belle Collaboration), *JHEP* **05**, 095 (2022)
- [28] W. Love *et al.* (CLEO Collaboration), *Phys. Rev. Lett.* **101**, 201601 (2008)
- [29] J. P. Lees *et al.* (BaBar Collaboration), *Phys. Rev. Lett.* **128**, 091804 (2022)
- [30] J. P. Lees *et al.* (BaBar Collaboration), *Phys. Rev. Lett.* **104**, 151802 (2010)

- [31] M. N. Achasov *et al.*, *Phys. Rev. D* **81**, 057102 (2010)
- [32] A. Salam and J. Strathdee, *Nucl. Phys. B* **87**, 85 (1975)
- [33] P. Fayet, *Nucl. Phys. B* **90**, 104 (1975)
- [34] G. D. Kribs, E. Poppitz, and N. Weiner, *Phys. Rev. D* **78**, 055010 (2008)
- [35] D. Stockinger, *J. Phys. G* **34**, R45 (2007)
- [36] T. Moroi, *Phys. Rev. D* **53**, 6565 (1996)
- [37] J. Hisano, T. Moroi, K. Tobe *et al.*, *Phys. Rev. D* **53**, 2442 (1996)
- [38] W. Kotlarski, D. Stöckinger, and H. Stöckinger-Kim, *JHEP* **08**, 082 (2019)
- [39] P. Diessner, J. Kalinowski, W. Kotlarski *et al.*, *JHEP* **12**, 124 (2014)
- [40] P. Diessner, J. Kalinowski, W. Kotlarski *et al.*, *Adv. High Energy Phys.* **2015**, 760729 (2015)
- [41] P. Diessner, J. Kalinowski, W. Kotlarski *et al.*, *JHEP* **03**, 007 (2016)
- [42] P. Diessner, W. Kotlarski, S. Liebschner *et al.*, *JHEP* **10**, 142 (2017)
- [43] P. Diessner and G. Weiglein, *JHEP* **07**, 011 (2019)
- [44] P. Diessner, J. Kalinowski, W. Kotlarski *et al.*, *JHEP* **09**, 120 (2019)
- [45] A. E. Blechman, *Mod. Phys. Lett. A* **24**, 633 (2009)
- [46] G. D. Kribs, A. Martin, and T. S. Roy, *JHEP* **06**, 042 (2009)
- [47] A. Kumar, D. Tucker-Smith, and N. Weiner, *JHEP* **09**, 111 (2010)
- [48] C. Frugiuele and T. Gregoire, *Phys. Rev. D* **85**, 015016 (2012)
- [49] S. Chakraborty, A. Chakraborty, and S. Raychaudhuri, *Phys. Rev. D* **94**, 035014 (2016)
- [50] J. Kalinowski, *Acta Phys. Polon. B* **47**, 203 (2016)
- [51] J. Braathen, M. D. Goodsell, and P. Slavich, *JHEP* **09**, 045 (2016)
- [52] P. Athron, J.-hyeon Park, T. Stuedtner *et al.*, *JHEP* **01**, 079 (2017)
- [53] P. Athron, M. Bach, D. H. J. Jacob *et al.*, *Phys. Rev. D* **106**, 095023 (2022)
- [54] C. Alvarado, A. Delgado, and A. Martin, *Phys. Rev. D* **97**, 115044 (2018)
- [55] K.-S. Sun, T. Guo, W. Li *et al.*, *Eur. Phys. J. C* **80**, 1167 (2020)
- [56] K.-S. Sun, S.-K. Cui, W. Li *et al.*, *Phys. Rev. D* **102**, 035029 (2020)
- [57] W. Porod, *Comput. Phys. Commun.* **153**, 275 (2003)
- [58] W. Porod and F. Staub, *Comput. Phys. Commun.* **183**, 2458 (2012)
- [59] W. Porod, F. Staub, and A. Vicente, *Eur. Phys. J. C* **74**, 2992 (2014)
- [60] F. Staub, *Adv. High Energy Phys.* **2015**, 840780 (2015)
- [61] F. Staub, arXiv: 0806.0538
- [62] F. Staub, *Comput. Phys. Commun.* **184**, 1792 (2013)
- [63] F. Staub, *Comput. Phys. Commun.* **185**, 1773 (2014)
- [64] P. A. Zyla *et al.* (Particle Data Group), *Prog. Theor. Exp. Phys.* **2020**, 083C01 (2020)
- [65] A. Khodjamirian, T. Mannel, and A. A. Petrov, *JHEP* **11**, 142 (2015)
- [66] T. A. Aaltonen *et al.* (CDF, D0 Collaboration), *Phys. Rev. D* **88**, 052018 (2013)
- [67] M. Aaboud *et al.* (ATLAS Collaboration), *Eur. Phys. J. C* **78**, 110 (2018)
- [68] R. Aaij *et al.* (LHCb Collaboration), *JHEP* **01**, 036 (2022)
- [69] T. Aaltonen *et al.* (CDF Collaboration), *Science* **376**, 170 (2022)
- [70] A. M. Baldini *et al.* (MEG Collaboration), *Eur. Phys. J. C* **78**, 380 (2018)
- [71] R. Fok and G. D. Kribs, *Phys. Rev. D* **82**, 035010 (2010)
- [72] M. Ablikim *et al.* (BESIII Collaboration), *Chin. Phys. C* **44**, 040001 (2020)